

# A VERY FAST, VERY STRONG, TOPOLOGICALLY MEANINGFUL AND FUN KNOT INVARIANT

DROR BAR-NATAN AND ROLAND VAN DER VEEN

ABSTRACT. In this paper we introduce  $\Theta = (\Delta, \theta)$ , a pair of polynomial knot invariants which is:

- Theoretically and practically fast:  $\Theta$  can be computed in polynomial time. We can compute it in full on random knots with over 300 crossings, and its evaluation at simple rational numbers on random knots with over 600 crossings.
- Strong: Its separation power is much greater than the hyperbolic volume, the HOMFLY-PT polynomial and Khovanov homology (taken together) on knots with up to 15 crossings (while being computable on much larger knots).
- Topologically meaningful: It gives a genus bound, and there are reasons to hope that it would do more.
- Fun: Scroll to Figures 1.1, 1.2, and 3.1.

$\Delta$  is merely the Alexander polynomial.  $\theta$  is almost certainly equal to an invariant that was studied extensively by Ohtsuki [Oh2], continuing Rozansky, Garoufalidis, and Kricker [GR, Ro1, Ro2, Ro3, Kr]. Yet our formulas, proofs, and programs are much simpler and enable its computation even on very large knots.

## CONTENTS

1. Fun	3
2. Formulas	7
2.1. Old Formulas	7
2.2. New Formulas	8
3. Implementation and Examples	11
3.1. Implementation	11
3.2. Examples	12
4. Proof of Invariance	17
5. Strong and Meaningful	27
5.1. Strong	27
5.2. Meaningful	28
6. Stories, Conjectures, and Dreams	31
References	33

*Date:* First edition Not Yet. This edition August 1, 2025.

*2020 Mathematics Subject Classification.* Primary 57K14, secondary 16T99.


*Key words and phrases.* Alexander polynomial, TBW.

This work was partially supported by NSERC grant RGPIN-2018-04350 and by the Chu Family Foundation (NYC). It is available in electronic form, along with source files and a demo *Mathematica* notebook at <http://drorbn.net/Theta> and at [arXiv:2508.00000](https://arxiv.org/abs/2508.00000).

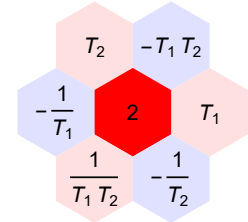


## 1. FUN

The word “fun” rarely appears in the title of a math paper, so let us start with a brief justification.

$\Theta$  is a pair of polynomials. The first,  $\Delta$ , is old news, the Alexander polynomial [Al]. It is a one-variable Laurent polynomial in a variable  $T$ . For example,  $\Delta(\textcircled{3}) = T^{-1} - 1 + T$ . We turn such a polynomial to a list of coefficients (for  $\textcircled{3}$ , it is  $(1 \ -1 \ 1)$ ), and then to a chain of bars of varying colours: white for the zero coefficients, and red and blue for the positive and negative coefficients (with intensity proportional to the magnitude of the coefficients). The result is a “bar code”, and for the trefoil  $\textcircled{3}$  is it .

Similarly,  $\theta$  is a 2-variable Laurent polynomial, in variables  $T_1$  and  $T_2$ . We can turn such a polynomial into a 2D array of coefficients and then using the same rules, into a 2D array of colours, namely, into a picture. To highlight a certain conjectured hexagonal symmetry of the resulting pictures, we apply a certain shear transformation to the plane before printing. So the colour of a monomial  $cT_1^{n_1}T_2^{n_2}$  gets printed at position  $\begin{pmatrix} 1 & -1/2 \\ 0 & \sqrt{3}/2 \end{pmatrix} \begin{pmatrix} n_1 \\ n_2 \end{pmatrix}$  instead of the more traditional  $\begin{pmatrix} n_1 \\ n_2 \end{pmatrix}$ . On the right is the 2D picture corresponding to the polynomial  $2 + T_1 - T_1T_2 + T_2 - T_1^{-1} + T_1^{-1}T_2^{-1} - T_2^{-1}$ .



Thus  $\Theta$  becomes a pair of pictures: a bar code, and a 2D picture that we call a “hexagonal QR code”. For the knots in the Rolfsen table (with the unknot prepended at the start), they are in Figure 1.1. In addition, the hexagonal QR codes of some 15 knots with  $\geq 300$  crossings are in Figure 1.2, and  $\Theta$  of a 132-crossing torus knot is in Figure 3.1.

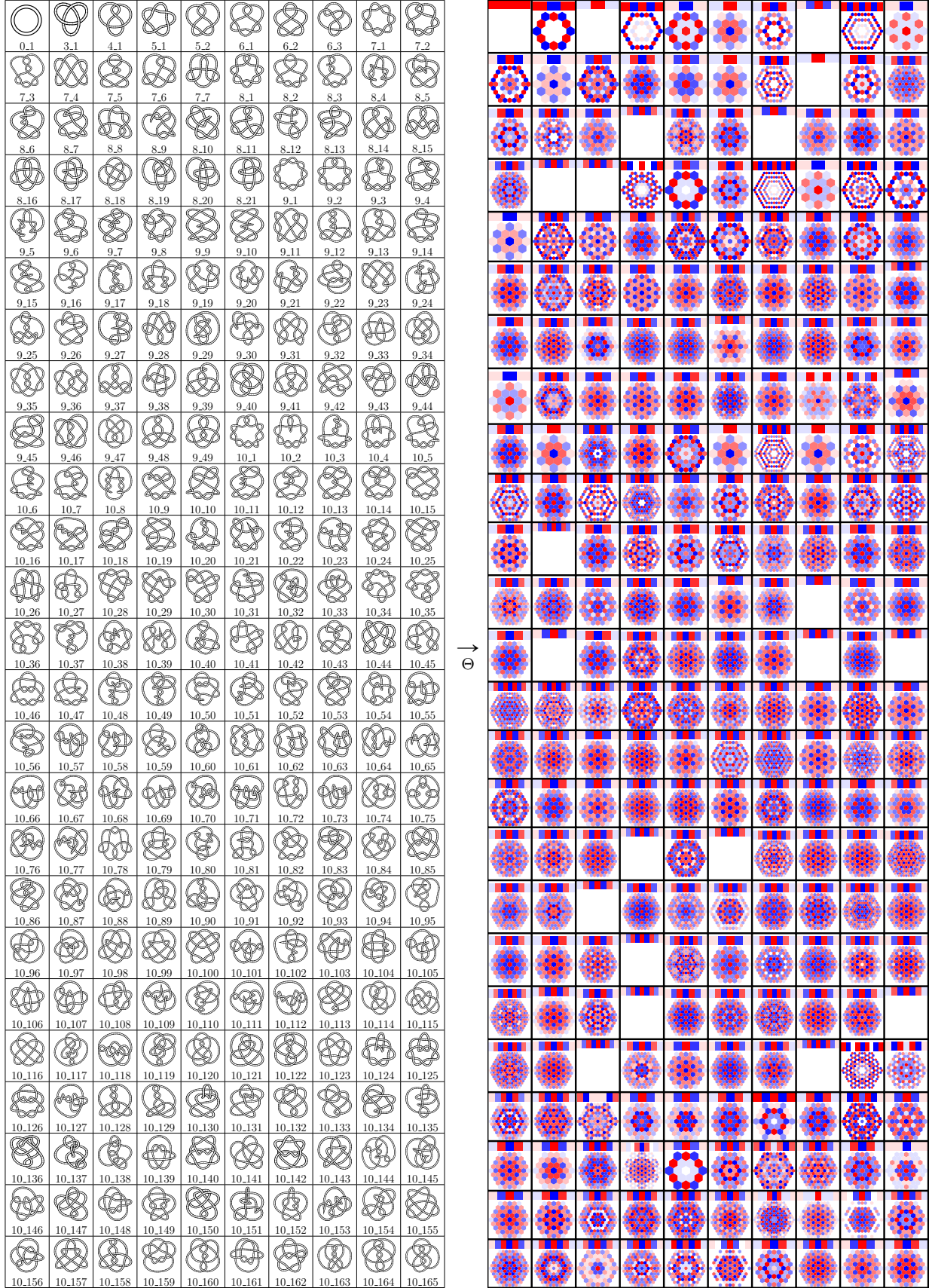
MORE. Add some mats.

Clearly there are patterns in these figures. There is a hexagonal symmetry and the QR codes are nearly always hexagons (these are independent properties). Much more can be seen in Figure 1.1. In Figure 1.2 there seem to be large-scale patterns perhaps reminiscent of the “Chladni figures” formed by powders atop vibrating plates (on right). We can’t prove any of these things, and the last one, we can’t even formulate properly. Yet they are clearly there, too clear to be the result of chance alone.



CC-BY-SA 4.0 / Wikimedia / Matematica (IME USP) / Rodrigo Tetsuo Argenton

We plan to have fun over the next few years observing and proving these patterns. We hope that others will join us too.

FIGURE 1.1.  $\Theta$  as a bar code and a QR code, for all the knots in the Rolfsen table.



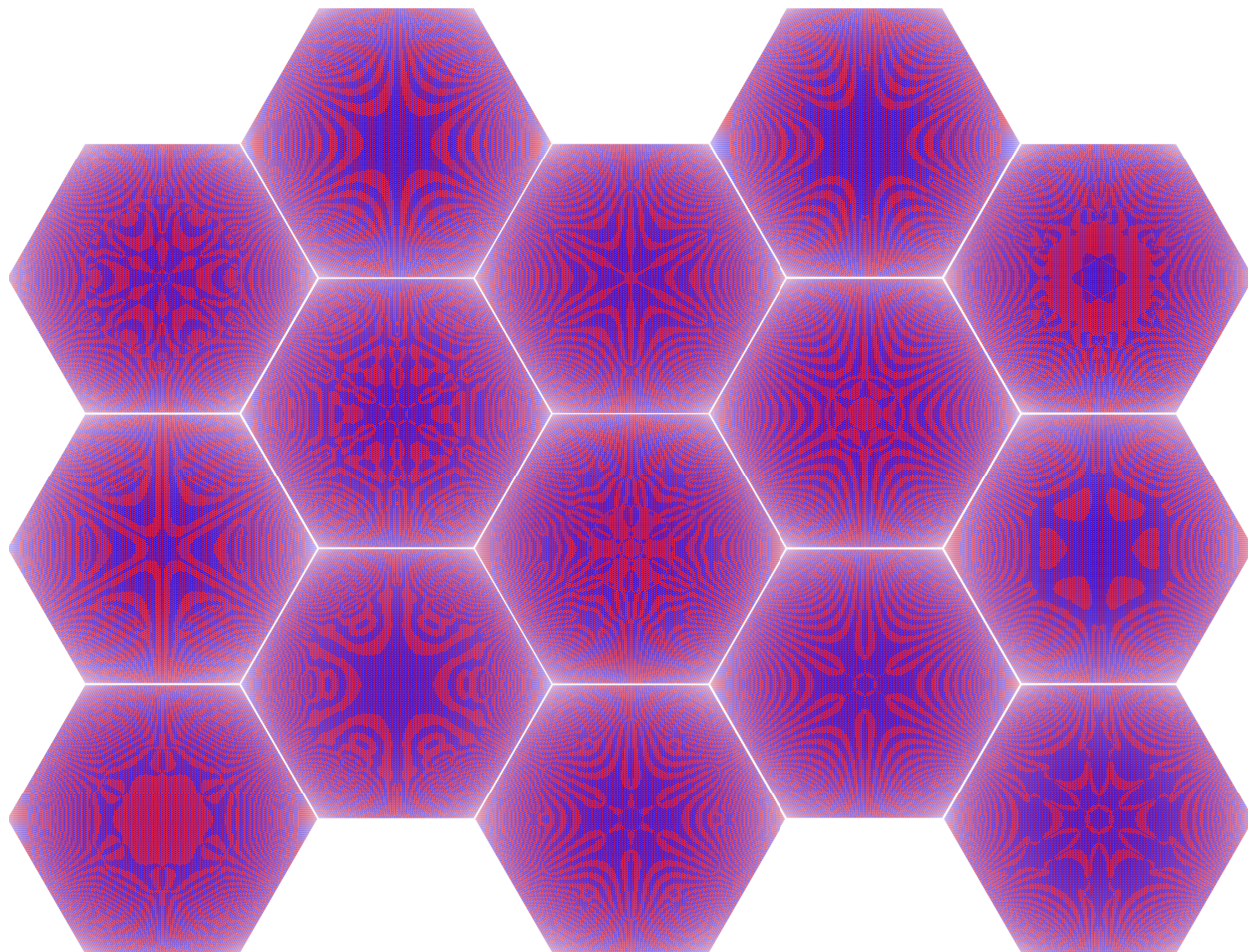


FIGURE 1.2.  $\theta$  (hexagonal QR code only) of the 15 largest knots that we have computed by September 16, 2024. They are all “generic” in as much as we know, and they all have  $\geq 300$  crossings. The knots come from [DHOEBL]. Warning: Some screens/printers may introduce spurious Moiré interference patterns.

fig:300

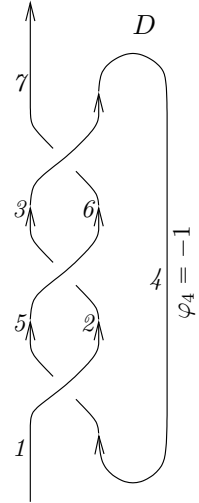


## 2. FORMULAS

**2.1. Old Formulas<sup>1</sup>.** The setup leading to the definition of  $\Theta$  is the same as the setup leading to the definition of the invariant  $\rho_1$  of [BV1], and hence we copy a few relevant paragraphs from [BV1] nearly verbatim, with only a few modifications.

Given an oriented  $n$ -crossing knot  $K$ , we draw it in the plane as a long knot diagram  $D$  in such a way that the two strands intersecting at each crossing are pointing up (that's always possible because we can always rotate crossings as needed), and so that at its beginning and at its end the knot is oriented upward. We call such a diagram an *upright knot diagram*. An example of an upright knot diagram is shown on the right.

We then label each edge of the diagram with two labels: a running index  $k$  which runs from 1 to  $2n + 1$ , and a “rotation number”  $\varphi_k$ , the geometric rotation number of that edge (the signed number of times the tangent to the edge is horizontal and heading right, with cups counted with  $+1$  signs and caps with  $-1$ ; this number is well defined because at their ends, all edges are headed up). On the right the running index runs from 1 to 7, and the rotation numbers for all edges are 0 (and hence are omitted) except for  $\varphi_4$ , which is  $-1$ .



**Technicality 1.** Some Reidemeister moves create or lose an edge and to avoid the need for renumbering it is beneficial to also allow labelling the edges with non-consecutive labels. Hence we allow that, and write  $i^+$  for the successor of the label  $i$  along the knot, and  $i^{++}$  for the successor of  $i^+$  (these are  $i + 1$  and  $i + 2$  if the labelling is by consecutive integers). Also, by convention “1” will always refer to the label of the first edge, and “ $2n + 1$ ” will always refer to the label of the last.

Let  $X$  be the set of all crossings in the diagram  $D$ , where we encode each crossing as a triple (sign, incoming over edge, incoming under edge). In our example we have  $X = \{(1, 1, 4), (1, 5, 2), (1, 3, 6)\}$ .

We let  $A$  be the  $(2n + 1) \times (2n + 1)$  matrix of Laurent polynomials in a formal variable  $T$ , defined by

$$A := I - \sum_{c=(s,i,j) \in X} (T^s E_{i,i^+} + (1 - T^s) E_{i,j^+} + E_{j,j^+}),$$

where  $I$  is the identity matrix and  $E_{\alpha\beta}$  denotes the elementary matrix with 1 in row  $\alpha$  and column  $\beta$  and zeros elsewhere.

Alternatively,  $A = I + \sum_c A_c$ , where  $A_c$  is a matrix of zeros except for the blocks as follows:

$$\begin{array}{c} \begin{array}{cc} j^+ \uparrow & i^+ \uparrow \\ \swarrow & \searrow \\ i & j \\ \swarrow & \searrow \\ j & i \\ s = +1 \end{array} & \begin{array}{cc} i^+ \uparrow & j^+ \uparrow \\ \swarrow & \searrow \\ j & i \\ \swarrow & \searrow \\ i & j \\ s = -1 \end{array} & \longrightarrow & \begin{array}{c|cc} A_c & \text{column } i^+ & \text{column } j^+ \\ \hline \text{row } i & -T^s & T^s - 1 \\ \text{row } j & 0 & -1 \end{array} \end{array} \quad (1)$$

We note (as we did in [BV1]) that the determinant of  $A$  is equal up to a unit to the normalized Alexander polynomial  $\Delta$  of  $K$ . In fact, we have that

$$\Delta = T^{(-\varphi(D) - w(D))/2} \det(A), \quad (2)$$

<sup>1</sup>“Old” means that these formulas appeared already in [BV1].

where  $\varphi(D) := \sum_k \varphi_k$  is the total rotation number of  $D$  and where  $w(D) = \sum_c s_c$  is the writhe of  $D$ , namely the sum of the signs  $s_c$  of all the crossings  $c$  in  $D$ .

We let  $G = (g_{\alpha\beta}) = A^{-1}$  and, thinking of it as a function  $g_{\alpha\beta}$  of a pair of edges  $\alpha$  and  $\beta$ , we call it the Green function of the diagram  $D$ . When inspired by physics (e.g. [BN3]) we sometimes call it “the 2-point function”, and when thinking of car traffic (e.g. [BV1, BN4]) we sometimes call it “the traffic function”.

We note that the computation of  $G$  is a bottleneck in the computation of  $\Theta$ . It requires inverting a  $(2n+1) \times (2n+1)$  matrix whose entries are (degree 1) Laurent polynomials in  $T$ . It's a daunting task yet it takes polynomial time, it can be performed in practice even if  $n$  is in the hundreds, and everything which then follows is easier.

MORE: Consider re-inserting traffic.

Discussion: A on next page

**2.2. New Formulas.** Let  $T_1$  and  $T_2$  be indeterminates and let  $T_3 := T_1 T_2$ . Let  $\Delta_\nu := \Delta|_{T \rightarrow T_\nu}$  and  $G_\nu = (g_{\nu\alpha\beta}) := G|_{T \rightarrow T_\nu}$  be  $\Delta$  and  $G$  subject to the substitution  $T \rightarrow T_\nu$ , where  $\nu = 1, 2, 3$  (these are easy to compute once  $\Delta$  and  $G$  have been computed).

Given crossings  $c = (s, i, j)$ ,  $c_0 = (s_0, i_0, j_0)$ , and  $c_1 = (s_1, i_1, j_1)$  in  $X$ , let

$$\begin{aligned} F_1(c) = & s [1/2 - g_{3ii} + T_2^s g_{1ii} g_{2ji} - T_2^s g_{3jj} g_{2ji} - (T_2^s - 1) g_{3ii} g_{2ji} \\ & + (T_3^s - 1) g_{2ji} g_{3ji} - g_{1ii} g_{2jj} + 2g_{3ii} g_{2jj} + g_{1ii} g_{3jj} - g_{2ii} g_{3jj}] \\ & + \frac{s}{T_2^s - 1} [(T_1^s - 1) T_2^s (g_{3jj} g_{1ji} - g_{2jj} g_{1ji} + T_2^s g_{1ji} g_{2ji}) \\ & + (T_3^s - 1) g_{3ji} (1 - T_2^s g_{1ii} + g_{2ij} + (T_2^s - 2) g_{2jj} - (T_1^s - 1)(T_2^s + 1) g_{1ji})] \end{aligned} \quad (3) \quad \text{eq:F1}$$

$$F_2(c_0, c_1) = \frac{s_1(T_1^{s_0} - 1)(T_3^{s_1} - 1)g_{1j_1i_0}g_{3j_0i_1}}{T_2^{s_1} - 1} (T_2^{s_0} g_{2i_1i_0} + g_{2j_1j_0} - T_2^{s_0} g_{2j_1i_0} - g_{2i_1j_0}) \quad (4) \quad \text{eq:F2}$$

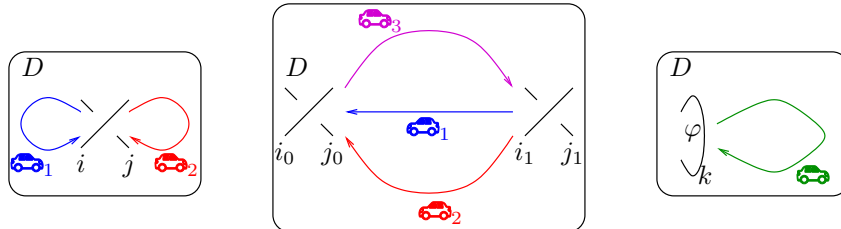
$$F_3(\varphi, k) = \varphi(g_{3kk} - 1/2) \quad (5) \quad \text{eq:F3}$$

These formulas are uninspiring, yet they are easy to compute (given  $G$ ), and they work:

**Theorem 2** (Proof in Section 4). *The following is a knot invariant:*

$$\theta(D) := \Delta_1 \Delta_2 \Delta_3 \left( \sum_{c \in X} F_1(c) + \sum_{c_0, c_1 \in X} F_2(c_0, c_1) + \sum_{\text{edges } k} F_3(\varphi_k, k) \right). \quad (6) \quad \text{eq:Main}$$

We note without detail that there is an alternative formula for  $\theta$  in terms of perturbed Gaussian integration [BN3]. In that language, and using also the traffic motifs of [BV1, BN4], the three summands in (6) become Feynman diagrams for processes in which cars governed by parameter  $T = T_1, T_2$ , or  $T_3$  interact:



In particular, the middle diagram which resembles the greek letter  $\Theta$  gave the invariant its name.

A VERY FAST, VERY STRONG, TOPOLOGICALLY MEANINGFUL AND FUN KNOT INVARIANT 9

We note also that computationally, the worst term in (6) <sup>leg:Main</sup> is the middle one, and even it takes merely  $\sim n^2$  operations in the ring  $\mathbb{Q}(T_1, T_2)$  to complete.

The polynomials  $F_1(c)$ ,  $F_2(c_0, c_1)$  and  $F_3(\varphi, k)$  are not unique, and we are not certain that we have the cleanest possible formulas for them. They are human-ugly, yet from a computational perspective, having 18 terms (as is the case for  $F_1(c)$ ) isn't really a problem; computers don't care.

✓ A: we note <sup>Following [APAF]</sup> ~~important~~ gap is...







## 3. IMPLEMENTATION AND EXAMPLES



**3.1. Implementation.** A concise yet reasonably efficient implementation is worth a thousand formulas. It completely removes ambiguities, it tests the theories, and it allows for experimentation. Hence our next task is to implement. The section that follows was generated from a Mathematica [Wo] notebook which is available at [BV3, Theta.nb]. A second implemtnation of  $\Theta$ , using Python and SageMath (<https://www.sagemath.org/>) is available at <https://www.rolandvdl.nl/Theta/>.

We start by loading the package `KnotTheory` — it is only needed because it has many specific knots pre-defined:

 `<< KnotTheory``  Loading KnotTheory` version of October 29, 2024, 10:29:52.1301.  
Read more at <http://katlas.org/wiki/KnotTheory>.


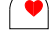
Next we quietly define the modules `Rot`, used to compute rotation numbers, and `PolyPlot`, used to plot polynomials as bar codes and as hexagonal QR codes. Neither is a part of the core of the computation of  $\Theta$ , so neither is shown; yet we do show one usage example for each.

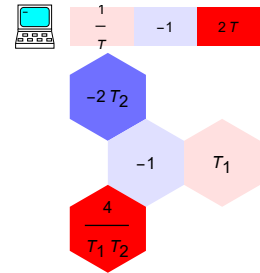
 `(* Rot suppressed *)`

 `Rot[Mirror@Knot[3, 1]]`  `{{{1, 1, 4}}, {1, 3, 6}}, {1, 5, 2}}, {0, 0, 0, -1, 0, 0, 0}}`


We urge the reader to compare the above output with the knot diagram in Section [2.1](#). [ssec:OldFormulas](#)

 `(* PolyPlot suppressed *)`


 `PolyPlot[{2 T - 1 + T-1, -1 + T1 - 2 T2 + 4 T1-1 T2-1},`  
 `ImageSize → 100, Labeled → True]`







The definition of `CF` below is a technicality telling the computer how to best store polynomials in the  $g_{\nu\alpha\beta}$ 's such as  $F_1$  and  $F_2$ . The programs would run just the same without it, albeit a bit more slowly:


 `CF[ $\mathcal{E}$ ] := Expand@Collect[ $\mathcal{E}$ ,  $g_{\_}$ , F] /. F → Factor;`

Next, we decree that  $T_3 = T_1 T_2$  and define the three “Feynman Diagram” polynomials  $F_1$ ,  $F_2$ , and  $F_3$ :



 `T3 = T1 T2;`

 `F1[{ $s_{\_}$ ,  $i_{\_}$ ,  $j_{\_}$ }] := CF[`  
  `$s \left( \frac{1}{2} - g_{3ii} + T_2^s g_{1ii} g_{2ji} - g_{1ii} g_{2jj} - (T_2^s - 1) g_{2ji} g_{3ii} + 2 g_{2jj} g_{3ii} - (1 - T_3^s) g_{2ji} g_{3ji} - \right.$`   
 `$g_{2ii} g_{3jj} - T_2^s g_{2ji} g_{3jj} + g_{1ii} g_{3jj} +$`   
 `$((T_1^s - 1) g_{1ji} (T_2^{2s} g_{2ji} - T_2^s g_{2jj} + T_2^s g_{3jj}) +$`   
 `$(T_3^s - 1) g_{3ji} (1 - T_2^s g_{1ii} + g_{2ij} + (T_2^s - 2) g_{2jj} - (T_1^s - 1) (T_2^s + 1) g_{1ji})) / (T_2^s - 1) \Big]$`

  $F_2[\{s\_, i\_, j\_ \}, \{s1\_, i1\_, j1\_ \}] :=$   
  $CF[s1 (T_1^{s\theta} - 1) (T_2^{s1} - 1)^{-1} (T_3^{s1} - 1) g_{1,j1,i\theta} g_{3,j\theta,i1}$   
 $( (T_2^{s\theta} g_{2,i1,i\theta} - g_{2,i1,j\theta}) - (T_2^{s\theta} g_{2,j1,i\theta} - g_{2,j1,j\theta})) ]$

  $F_3[\varphi\_, k\_] = \varphi g_{3kk} - \varphi / 2;$


Next comes the main program computing  $\Theta$ . Fortunately, it matches perfectly with the mathematical description in Section 2. In line 01 we let  $X$  be the list of crossings in an input knot  $K$ , and  $\varphi$  the list of its rotation numbers, using the external program **Rot** which we have already mentioned. We also let  $n$  be the length of  $X$ , namely, the number of crossings in  $K$ . In line 02 we let the starting value of  $A$  be the identity matrix, and then in line 03, for each crossing in  $X$  we add to  $A$  a  $2 \times 2$  block, in rows  $i$  and  $j$  and columns  $i + 1$  and  $j + 1$ , as explain in Equation (1). In line 04 we compute the normalized Alexander polynomial  $\Delta$  as in (2). In line 05 we let  $G$  be the inverse of  $A$ . In line 06 we declare what it means to evaluate, **ev**, a formula  $\mathcal{E}$  that may contain symbols of the form  $g_{\nu\alpha\beta}$ : each such symbol is to be replaced by the entry in position  $\alpha, \beta$  of  $G$ , but with  $T$  replaced with  $T_\nu$ . In line 07 we start computing  $\theta$  by computing the first summand in (6), which in itself, is a sum over the crossings of the knot. In line 08 we add to  $\theta$  the double sum corresponding to the second term in (6), and in line 09, we add the third summand of (6). Finally, line 10 outputs a pair:  $\Delta$ , and the re-normalized version of  $\theta$ .

  $\Theta[K\_]:= \Theta[K] = \text{Module}[\{X, \varphi, n, A, \Delta, G, \text{ev}, \theta\},$   
  $( * 01 * ) \{X, \varphi\} = \text{Rot}[K]; n = \text{Length}[X];$   
 $( * 02 * ) A = \text{IdentityMatrix}[2 n + 1];$   
 $( * 03 * ) \text{Cases}[X, \{s\_, i\_, j\_ \} \Rightarrow (A[[\{i, j\}, \{i + 1, j + 1\}]] += \begin{pmatrix} -T^s & T^s - 1 \\ \theta & -1 \end{pmatrix})];$   
 $( * 04 * ) \Delta = T^{(-\text{Total}[\varphi] - \text{Total}[X[[\text{All}, 1]]]) / 2} \text{Det}[A];$   
 $( * 05 * ) G = \text{Inverse}[A];$   
 $( * 06 * ) \text{ev}[\mathcal{E}\_] := \text{Factor}[\mathcal{E} /. g_{\nu, \alpha, \beta} \Rightarrow (G[[\alpha, \beta]] /. T \rightarrow T_\nu)];$   
 $( * 07 * ) \theta = \text{ev}[\sum_{k=1}^n F_1[X[[k]]];$   
 $( * 08 * ) \theta += \text{ev}[\sum_{k1=1}^n \sum_{k2=1}^n F_2[X[[k1]], X[[k2]]];$   
 $( * 09 * ) \theta += \text{ev}[\sum_{k=1}^{2n} F_3[\varphi[[k]], k];$   
 $( * 10 * ) \text{Factor}@\{\Delta, (\Delta /. T \rightarrow T_1) (\Delta /. T \rightarrow T_2) (\Delta /. T \rightarrow T_3) \theta\}$   
 $];$


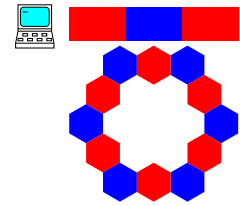
c:Examples

3.2. **Examples.** On to examples! Starting with the trefoil knot.

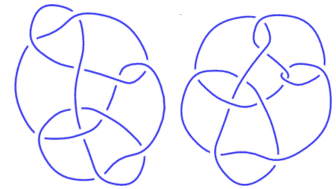

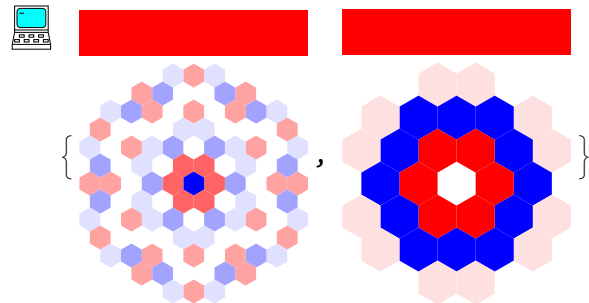
  $\text{Expand}[\Theta[\text{Knot}[3, 1]]]$

  $\left\{ -1 + \frac{1}{T} + T, -\frac{1}{T_1^2} - T_1^2 - \frac{1}{T_2^2} - \frac{1}{T_1^2 T_2^2} + \frac{1}{T_1 T_2^2} + \frac{1}{T_1^2 T_2} + \frac{T_1}{T_2} + \frac{T_2}{T_1} + T_1^2 T_2 - T_2^2 + T_1 T_2^2 - T_1^2 T_2^2 \right\}$




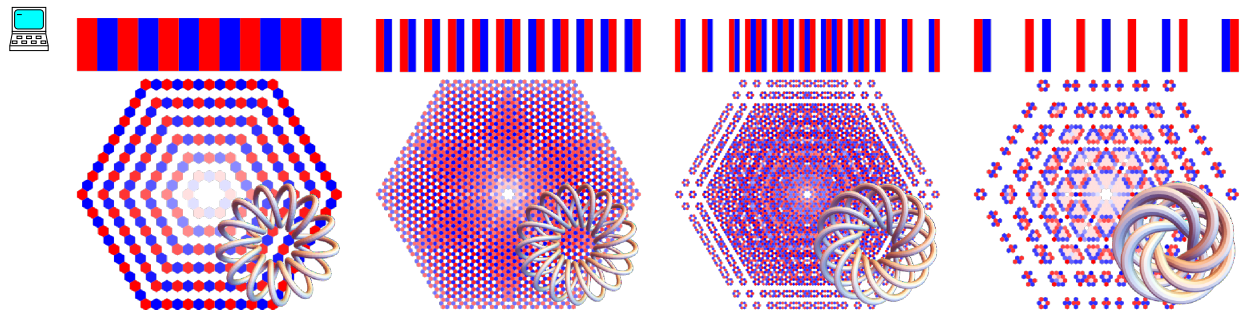
A VERY FAST, VERY STRONG, TOPOLOGICALLY MEANINGFUL AND FUN KNOT INVARIANT 13

 `PolyPlot[ $\Theta$ [Knot[3, 1]], ImageSize  $\rightarrow$  Tiny]`



Next are the Conway knot  $11_{n34}$  and the Kinoshita-Terasaka knot  $11_{n42}$ . The two are mutants and famously hard to separate: they both have  $\Delta = 1$  (as evidenced by their one-bar Alexander bar codes below), and they have the same hyperbolic volume, HOMFLY-PT polynomial, and Khovanov homology. Yet their  $\theta$  invariants are different. Note that the genus of the Conway knot is 3, while the genus of the Kinoshita-Terasaka knot is 2. This agrees with the apparent higher complexity of the QR code of the Conway polynomial and with Conjecture 14 below.


 `PolyPlot[ $\Theta$ [Knot[#]], ImageSize  $\rightarrow$  120] & /@ {"K11n34", "K11n42"}`


Torus knots have particularly nice-looking  $\Theta$  invariants. Here are the torus knots  $T_{13/2}$ ,  $T_{17/3}$ ,  $T_{13/5}$ , and  $T_{7/6}$ :

 `GraphicsRow[ImageCompose[  
 PolyPlot[ $\Theta$ [TorusKnot @@ #], ImageSize  $\rightarrow$  480],  
 TubePlot[TorusKnot @@ #, ImageSize  $\rightarrow$  240],  
{Right, Bottom}, {Right, Bottom}  
] & /@ {{13, 2}, {17, 3}, {13, 5}, {7, 6}}]`

The next line shows the computation time in seconds for the 132-crossing torus knot  $T_{22/7}$  on a 2024 laptop, without actually showing the output. The output plot is in Figure 3.1.

 `AbsoluteTiming[ $\Theta$ [TorusKnot[22, 7]]];`
 {1020.73, Null}

```
ImageCompose[PolyPlot[Θ[TorusKnot[22, 7]], ImageSize → 720],  
TubePlot[TorusKnot[22, 7], ImageSize → 360], {Right, Bottom}, {Right, Bottom}]
```

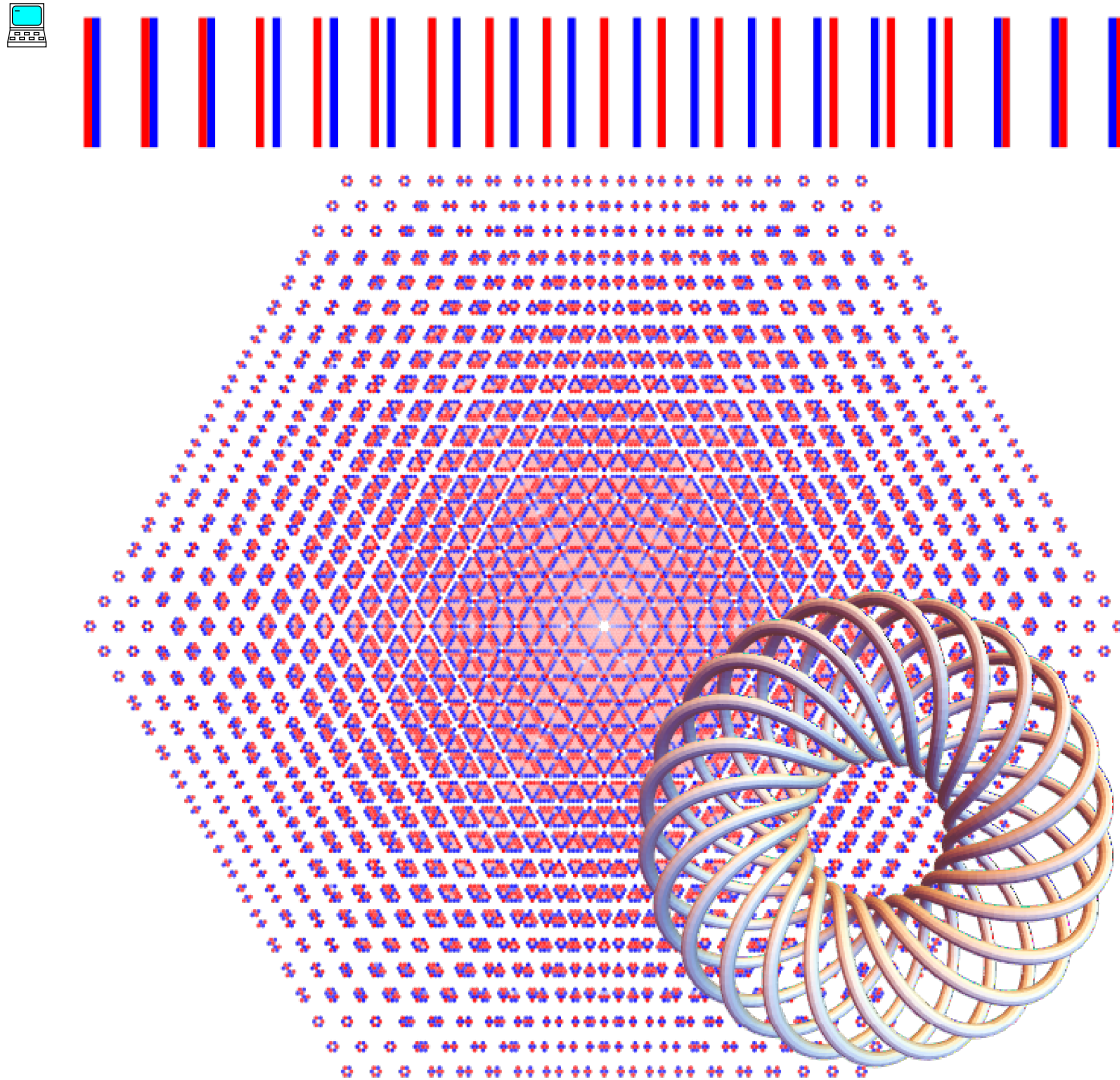


FIGURE 3.1. The 132-crossing torus knot  $T_{22/7}$  and a plot of its  $\Theta$  invariant

We note that if  $T_1$  and  $T_2$  are assigned specific rational numbers and if the program for  $\Theta$  is slightly modified so as to compute each  $G_\nu$  separately (rather than computing  $G$  symbolically and then substituting  $T \Rightarrow T_\nu$ ), then the program becomes significantly more efficient, for inverting a numerical matrix is cheaper than inverting a symbolic matrix (but then one obtains numerical answers and the beauty and the topological significance (Section 5) are lost). The Mathematica notebook that accompanies this paper, [BV3, Theta.nb], contains the required modified program as well as a few computational examples. One finds that with  $T_1 = 22/7$  and  $T_2 = 21/13$ , the invariant  $\Theta$  can be computed for knots with 600 crossings, and that for knots with up to 15 crossings, its separation power remains the same.

If  $T_1$  and  $T_2$  are assigned approximate real values, say  $\pi$  and  $e$  computed to 100 decimal digits, then  $\Theta$  can be computed on knots with 1,000 crossings and, for knots with up to 15



A VERY FAST, VERY STRONG, TOPOLOGICALLY MEANINGFUL AND FUN KNOT INVARIANT 15

crossings it remains very strong. But approximate real numbers are a bit thorny. It is hard to know how far one needs to compute before deciding that two such numbers are equal, and when two such numbers appear unequal, it is hard to tell if that is merely because they were computed differently and different roundings were applied. Thorns and snares are in the way of the perverse; He who guards his soul will be far from them (Proverbs 22:5)<sup>2</sup>.

---

<sup>2</sup> שומר נפשו ירחק.



## 4. PROOF OF INVARIANCE

Our proof of the invariance of  $\theta$  (Theorem 2) is very similar, and uses many of the same pieces, as the proof of the invariance of  $\rho_1$  in [BV1]. Thus at some places here we are briefer than at [BV1], and sadly, yet in the interest of saving space, we ~~completely omit~~ here the interpretation of  $g_{\alpha\beta}$  as a “traffic function”. *isn't it subtle*

Like in [BV1, Lemma 3], the equalities  $AG = I$  and  $GA = I$  imply that for any crossing  $c = (s, i, j)$  in a knot diagram  $D$ , the Green function  $G = (g_{\alpha\beta})$  of  $D$  satisfies the following “ $g$ -rules”, with  $\delta$  denoting the Kronecker delta:

$$g_{i\beta} = \delta_{i\beta} + T^s g_{i^+, \beta} + (1 - T^s) g_{j^+, \beta}, \quad g_{j\beta} = \delta_{j\beta} + g_{j^+, \beta}, \quad g_{2n+1, \beta} = \delta_{2n+1, \beta}, \quad (7)$$

$$g_{\alpha, i^+} = T^s g_{\alpha i} + \delta_{\alpha, i^+}, \quad g_{\alpha, j^+} = g_{\alpha j} + (1 - T^s) g_{\alpha i} + \delta_{\alpha, j^+}, \quad g_{\alpha, 1} = \delta_{\alpha, 1}. \quad (8)$$

Furthermore, the systems of equations (7) is equivalent to  $AG = I$  and so it fully determines  $g_{\alpha\beta}$ , and likewise for the system (8), which is equivalent to  $GA = I$ .

Of course, the same  $g$ -rules also hold for  $G_\nu = (g_{\nu\alpha\beta})$  for  $\nu = 1, 2, 3$ , except with  $T$  replaced with  $T_\nu$ .

We also need a variant  $\tilde{g}_{ab}$  of  $g_{\alpha\beta}$ , defined whenever  $a$  and  $b$  are two distinct points on the edges of a knot diagram  $D$ , away from the crossings. If  $\alpha$  is the edge on which  $a$  lies and  $\beta$  is the edge on which  $b$  lies,  $\tilde{g}_{ab}$  is defined as follows:

$$\tilde{g}_{ab} = \begin{cases} g_{\alpha\beta} & \text{if } \alpha \neq \beta, \\ g_{\alpha\beta} & \text{if } \alpha = \beta \text{ and } a < b \text{ relative to the orientation of the edge } \alpha = \beta, \\ g_{\alpha\beta} - 1 & \text{if } \alpha = \beta \text{ and } a > b \text{ relative to the orientation of the edge } \alpha = \beta. \end{cases} \quad (9)$$

Of course, we can define  $\tilde{g}_{\nu ab}$  from  $g_{\alpha\beta}$  in a similar way.

It is clear that  $g$  and  $\tilde{g}$  contain the same information and are easily computable from each other. The variant  $\tilde{g}$  is, strictly speaking, not a matrix and so  $g$  is a bit more suitable for computations. Yet  $\tilde{g}$  is a bit better behaved when we try to track, as below, the behaviour of  $g / \tilde{g}$  under Reidemeister moves. Reidemeister moves sometimes merge two edges into one or break an edge into two. In such cases the points  $a$  and  $b$  can be “pulled” along with the move so as to retain their ordering along the overall parametrization of the knot, yet mere edge labels lose this information. The following discussion and lemma exemplify the advantage of  $\tilde{g}$  of  $g$ :

**Discussion 3.** We introduce “null vertices” as on the right into knot diagrams, whose only function (as we shall see) is to cut edges into parts that may carry different labels. When dealing with upright knot diagrams as in Section 2.1, we only allow null vertices where the tangent to the knot is pointing up, so that the rotation numbers  $\varphi_k$  remain well defined on all edges. In the presence of null vertices the matrix  $A$  becomes a bit larger (by as many null vertices as were added to a knot diagram). The rule (1) for the creation of the matrix  $A$  gets an amendment for null vertices,

$$\begin{array}{c} j \quad k \\ \bullet \end{array} \longrightarrow \longrightarrow \frac{A_{nv} \mid \text{column } k}{\text{row } j \mid -1},$$

and the summation for  $A$ ,  $A = I + \sum_c A_c + \sum_{nv} A_{nv}$  is extended to include summands for the null vertices. The matrix  $G = A^{-1}$  and the function  $g_{\alpha\beta}$  are defined as before. The  $g$ -rules of (7) and (8) get additions,

*A: From the perspective of traffic functions,  $\tilde{g}_{\alpha\beta}$  is a bit more natural than  $g_{\alpha\beta}$  as it avoids the ad hoc decree that for  $\alpha = \beta$  ...*

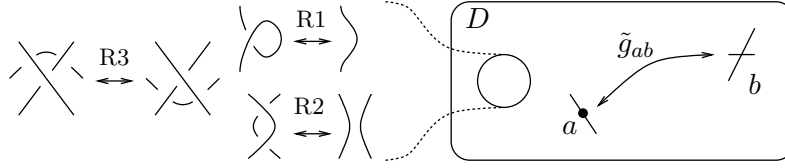


FIGURE 4.1. The modified Green function  $\tilde{g}_{ab}$  is invariant under Reidemeister moves performed away from where it is measured.

$$g_{j\beta} = \delta_{j\beta} + g_{k\beta},$$

(10)

$$\text{eq:NullCov} \text{ and } g_{\alpha k} = \delta_{\alpha k} + g_{\alpha j},$$

(11)

$$\text{eq:NullCov}$$

and it remains true that the system of equations (7)  $\cup$  (10) (as well as (8)  $\cup$  (11)) fully determines  $g_{\alpha\beta}$ . The variant  $\tilde{g}_{ab}$  is also defined as before, except now  $a$  and  $b$  need to also be away from the null vertices.

**Lemma 4.** *Inserting a null vertex does not change  $\tilde{g}_{ab}$  provided it is inserted away from  $a$  and  $b$ . (This statement does not make sense for  $g_{\alpha\beta}$ , as inserting a null vertex changes the dimensions of the matrix  $G = (g_{\alpha\beta})$ ).*

*Proof.* Let  $D$  be an upright knot diagram having an edge labeled  $i$  and let  $D'$  be obtained from it by adding a null vertex within edge  $i$ , naming the two resulting half-edges  $j$  and  $k$  (in order). Let  $g_{\alpha\beta}$  be the Green function for  $D$ , and similarly,  $g'_{\alpha\beta}$  for  $D'$ . We claim that

$$g'_{\alpha\beta} = \begin{array}{c|ccc} & \beta = j & \beta = k & \beta \notin \{j, k\} \\ \hline \alpha = j & g_{ii} & g_{ii} & g_{i\beta} \\ \alpha = k & g_{ii} - 1 & g_{ii} & g_{i\beta} \\ \alpha \notin \{j, k\} & g_{\alpha i} & g_{\alpha i} & g_{\alpha\beta} \end{array}.$$

Indeed, all we have to do is to verify that the above-defined  $g'_{\alpha\beta}$  satisfies all the  $g$ -rules (7)  $\cup$  (10), and that is easy. The lemma now follows easily from the definition of  $\tilde{g}'$  in Equation (9).  $\square$

**Remark 5.** The statement of Theorem 2 does not change in the presence of null vertices: There are no “ $F$ ” terms for those, and their only effect on the definition of  $\Theta$  in Equation (6) is to change the edge labels that appear within  $c$ ,  $c_1$ , and  $c_2$ , and within the  $F_3$  sum.

The following theorem was not named in [BV1] yet it was stated there as the first part of the first proof of [BV1, Theorem 1].

**Theorem 6.** *The variant Green function  $\tilde{g}_{ab}$  is a “relative invariant”, meaning that once points  $a$  and  $b$  are fixed within a knot diagram  $D$ , the value of  $\tilde{g}_{ab}$  does not change if Reidemeister moves are performed away from the points  $a$  and  $b$ . An illustration appears in Figure 4.1. It follows that the same is also true for  $\tilde{g}_{\nu ab}$  for  $\nu = 1, 2, 3$ .*

We note that  $\tilde{g}_{ab}$  is nearly the same as  $g_{\alpha\beta}$ , if  $a$  is on  $\alpha$  and  $b$  is on  $\beta$ . So Theorem 6 also says that  $g_{\alpha\beta}$  is invariant under Reidemeister moves away from  $\alpha$  and  $\beta$ , except for edge-renumbering issues and  $\pm 1$  contributions that arise if  $\alpha$  and  $\beta$  correspond to edge that get merged or broken by the Reidemeister moves.

The proof of Theorem 6 is perhaps best understood in terms of the traffic function of [BV1, BV2, BN4]: One simply needs to verify that for each of the Reidemeister moves, traffic entering the tangle diagram for the left hand side of the move exits it in the same manner

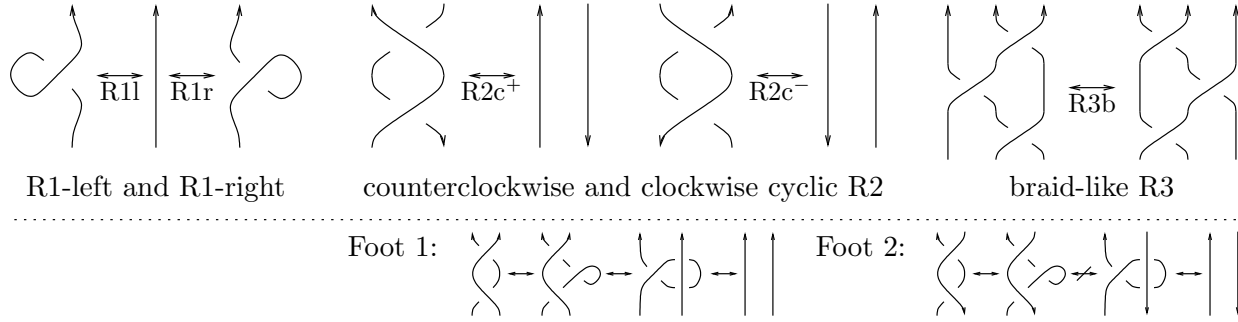


FIGURE 4.2. A generating set of oriented Reidemeister moves as in [Po, Figure 6]. Foot 1: the braid-like R2b is not needed. Foot 2: yet R2b cannot replace  $R2c^\pm$  because in the would-be proof, an unpostulated form of R3 is used (which in itself follows from  $R2c^\pm$ ).

as traffic entering the tangle diagram for the right hand side of the move, and each of these verifications, as explained in [BV1, BN2, BN4], is very easy. Yet that proof is a bit informal, so we opt here to give a fully formal proof along the lines of the first halves of [BV1, Propositions 7-9].

*Proof of Theorem 6.* We need to know how the Green function  $g_{\alpha\beta}$  changes under the orientation-sensitive Reidemeister moves of Figure 4.2 (note that the  $g_{\alpha\beta}$  do not see the rotation numbers and don't care if a knot diagram is upright in the sense of Section 2.1).

We start with R3b. Below are the two sides of the move, along with the  $g$ -rules of type (7) corresponding to the crossings within, written with the assumption that  $\beta$  isn't in  $\{i^+, j^+, k^+\}$ , so several of the Kronecker deltas can be ignored. We use  $g$  for the Green function at the left-hand side of R3b, and  $g'$  for the right-hand side, and recall that along with the further  $g/g'$ -rules corresponding to all the non-moving knot crossings, these rules fully determine  $g_{\alpha\beta}$  and  $g'_{\alpha\beta}$  for  $\beta \notin \{i^+, j^+, k^+\}$ :

	$g_{i^+, \beta} = T g_{i^{++}, \beta} + (1-T) g_{j^{++}, \beta}$ $g_{j^+, \beta} = g_{j^{++}, \beta}$ $g_{i, \beta} = \delta_{i\beta} + T g_{i^+, \beta} + (1-T) g_{k^{++}, \beta}$ $g_{k^+, \beta} = g_{k^{++}, \beta}$ $g_{j, \beta} = \delta_{j\beta} + T g_{j^+, \beta} + (1-T) g_{k^+, \beta}$ $g_{k, \beta} = \delta_{k\beta} + g_{k^+, \beta}$		$g'_{j^+, \beta} = T g'_{j^{++}, \beta} + (1-T) g'_{k^{++}, \beta}$ $g'_{k^+, \beta} = g'_{k^{++}, \beta}$ $g'_{i^+, \beta} = T g'_{i^{++}, \beta} + (1-T) g'_{k^+, \beta}$ $g'_{k, \beta} = \delta_{k\beta} + g'_{k^+, \beta}$ $g'_{i, \beta} = \delta_{i\beta} + T g'_{i^+, \beta} + (1-T) g'_{j^+, \beta}$ $g'_{j, \beta} = \delta_{j\beta} + g'_{j^+, \beta}$
...	...	...	...
further crossings	further $g$ -rules	further crossings	further $g'$ -rules

A routine computation (eliminating  $g_{i^+, \beta}$ ,  $g_{j^+, \beta}$ , and  $g_{k^+, \beta}$ ) shows that the first system of 6 equations is equivalent to the following system of 6 equations:

$$\begin{aligned} g_{i, \beta} &= \delta_{i\beta} + T^2 g_{i^{++}, \beta} + T(1-T) g_{j^{++}, \beta} + (1-T) g_{k^{++}, \beta}, \\ g_{j, \beta} &= \delta_{j\beta} + T g_{j^{++}, \beta} + (1-T) g_{k^{++}, \beta}, & g_{k, \beta} &= \delta_{k\beta} + g_{k^{++}, \beta}, \end{aligned} \quad (12)$$

$$g_{i^+, \beta} = T g_{i^{++}, \beta} + (1-T) g_{j^{++}, \beta}, \quad g_{j^+, \beta} = g_{j^{++}, \beta}, \quad g_{k^+, \beta} = g_{k^{++}, \beta}. \quad (13)$$



In this system the indices  $i^+$ ,  $j^+$  and  $k^+$  do not appear in (12) or in the further  $g$ -rules corresponding to the further crossings. Hence for the purpose of determining  $g_{\alpha\beta}$  with  $\alpha, \beta \notin \{i^+, j^+, k^+\}$ , Equations (13) can be ignored.

Similarly eliminating  $g'_{i^+, \beta}$ ,  $g'_{j^+, \beta}$ , and  $g'_{k^+, \beta}$  from the second set of equations, we find that it is equivalent to

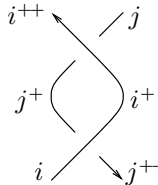
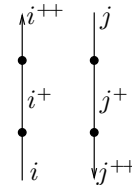
$$\begin{aligned} g'_{i, \beta} &= \delta_{i\beta} + T^2 g'_{i^{++}, \beta} + T(1-T)g'_{j^{++}, \beta} + (1-T)g'_{k^{++}, \beta}, \\ g'_{j, \beta} &= \delta_{j\beta} + Tg'_{j^{++}, \beta} + (1-T)g'_{k^{++}, \beta}, \quad g'_{k, \beta} = \delta_{k\beta} + g'_{k^{++}, \beta}, \end{aligned} \quad (14)$$

$$g'_{i^+, \beta} = Tg'_{i^{++}, \beta} + (1-T)g'_{k^{++}, \beta}, \quad g'_{j^+, \beta} = Tg'_{j^{++}, \beta} + (1-T)g'_{k^{++}, \beta}, \quad g'_{k^+, \beta} = g'_{k^{++}, \beta}. \quad (15)$$

Using the same logic as before, for the purpose of determining  $g'_{\alpha\beta}$  with  $\alpha, \beta \notin \{i^+, j^+, k^+\}$ , Equations (15) can be ignored.

But now we compare the unignored equations, (12) and (14), and find that they are exactly the same, except with  $g \leftrightarrow g'$ , and the same is true for the further  $g/g'$ -rules coming from the further crossings. Hence so long as  $\alpha, \beta \notin \{i^+, j^+, k^+\}$ , we have that  $g_{\alpha\beta} = g'_{\alpha\beta}$ . In the case of the R3b move no edges merge or break up, and hence this implies that  $\tilde{g}_{ab} = \tilde{g}'_{ab}$  so long as  $a$  and  $b$  are away from the move.

Next we deal with the case of R2c<sup>+</sup>. We use the privileges afforded to us by Lemma 4 to insert 4 null vertices into the right-hand-side of the move, and like in the case of R3b, we start with pictures annotated with the relevant type (7) and (10)  $g$ -rules, written with the assumption that  $\beta \notin \{i^+, j^+\}$ :

	$\begin{aligned} g_{i^+, \beta} &= Tg_{i^{++}, \beta} + (1-T)g_{j^+, \beta} \\ g_{j, \beta} &= \delta_{j, \beta} + g_{j^+, \beta} \\ g_{i, \beta} &= \delta_{i, \beta} + T^{-1}g_{i^+, \beta} + (1-T^{-1})g_{j^{++}, \beta} \\ g_{j^+, \beta} &= g_{j^{++}, \beta} \end{aligned}$		$\begin{aligned} g'_{i, \beta} &= \delta_{i, \beta} + g'_{i^+, \beta} \\ g'_{j^+, \beta} &= g'_{j^{++}, \beta} \\ g'_{i^+, \beta} &= g'_{i^{++}, \beta} \\ g'_{j, \beta} &= \delta_{j, \beta} + g'_{j^+, \beta} \end{aligned}$
...		...	
further crossings	further $g$ -rules	further crossings	further $g'$ -rules

As in the case of R3b, we eliminate  $g_{i^+, \beta}$  and  $g_{j^+, \beta}$  from the equations for the left hand side, and find that for the purpose of determining  $g_{\alpha\beta}$  with  $\beta \notin \{i^+, j^+\}$ , they are equivalent to the equations

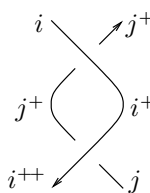
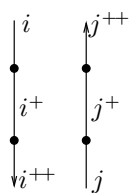
$$g_{i, \beta} = \delta_{i, \beta} + g_{i^{++}, \beta} \quad \text{and} \quad g_{j, \beta} = \delta_{j, \beta} + g_{j^{++}, \beta}.$$

Likewise, the right hand side is clearly equivalent to

$$g'_{i, \beta} = \delta_{i, \beta} + g'_{i^{++}, \beta} \quad \text{and} \quad g'_{j, \beta} = \delta_{j, \beta} + g'_{j^{++}, \beta},$$

and as in the case of R3b, this establishes the invariance of  $\tilde{g}_{ab}$  under R2c moves.

For the remaining moves, R2c<sup>-</sup>, R1l, and R1r, we merely display the  $g$ -rules and leave it to the readers to verify that when the edges  $i^+$  and/or  $j^+$  are eliminated, the left hand sides become equivalent to the right hand sides:

	$\begin{aligned} g_{i, \beta} &= \delta_{i, \beta} + Tg_{i^+, \beta} + (1-T)g_{j^{++}, \beta} \\ g_{j^+, \beta} &= g_{j^{++}, \beta} \\ g_{i^+, \beta} &= T^{-1}g_{i^{++}, \beta} + (1-T^{-1})g_{j^+, \beta} \\ g_{j, \beta} &= \delta_{j, \beta} + g_{j^+, \beta} \end{aligned}$		$\begin{aligned} g'_{i, \beta} &= \delta_{i, \beta} + g'_{i^+, \beta} \\ g'_{j^+, \beta} &= g'_{j^{++}, \beta} \\ g'_{i^+, \beta} &= g'_{i^{++}, \beta} \\ g'_{j, \beta} &= \delta_{j, \beta} + g'_{j^+, \beta} \end{aligned}$
---	---	--	--

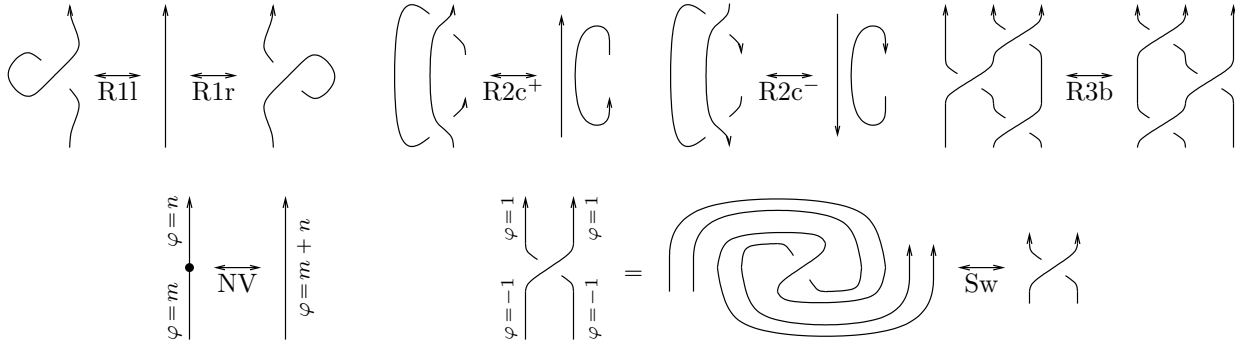


FIGURE 4.3. The upright Reidemeister moves: The R1 and R3 moves are already upright, and remain the same as in Figure 4.2. The crossings in the R2 moves of Figure 4.2 are rotated to be upright. We also need two further moves: The null vertex move NV for adding and removing null vertices, and the swirl move Sw which then implies that any two ways of turning a crossing upright are the same. We sometimes indicate rotation numbers symbolically rather than using complicated spirals.

$$\begin{array}{ccc}
 \begin{array}{c} i^{++} \\ \text{loop} \\ i \end{array} & \begin{array}{l} g_{i^+, \beta} = T g_{i^{++}, \beta} \\ \quad + (1 - T) g_{i^+, \beta} \\ g_{i, \beta} = \delta_{i, \beta} + g_{i^+, \beta} \end{array} & \begin{array}{c} i^{++} \\ \text{loop} \\ i \end{array} & \begin{array}{l} g'_{i^+, \beta} = g'_{i^{++}, \beta} \\ g'_{i, \beta} = \delta_{i, \beta} + g'_{i^+, \beta} \end{array} & \begin{array}{c} i^{++} \\ \text{loop} \\ i \end{array} & \begin{array}{l} g''_{i^+, \beta} = g''_{i^{++}, \beta} \\ g''_{i, \beta} = \delta_{i, \beta} + T g''_{i^+, \beta} \\ \quad + (1 - T) g''_{i^{++}, \beta} \end{array}
 \end{array}$$

We can now move on to the main part of the proof of Theorem 2. We need to show the invariance of  $\theta$  under the “upright Reidemeister” moves of Figure 4.3.

**Proposition 7.** *The moves in Figure 4.3 are sufficient. If two upright knot diagrams (with null vertices) represent the same knot, they can be connected by a sequence of moves as in the figure.*

*Proof.* The proof is essentially contained in the caption of Figure 4.3. A more detailed version is in [BVH].  $\square$

**Proposition 8.** *The quantity  $\theta$  is invariant under R3b.*

*Proof.* Let  $D_l$  and  $D_r$  be two knot diagrams that differ only by an R3b move, and label their relevant edges and crossings as in Figure 4.4. Let  $g_{\nu\alpha\beta}^l$  and  $g_{\nu\alpha\beta}^r$  be their corresponding Green functions. Let  $F_1^l(c)$ ,  $F_2^l(c_0, c_1)$  and  $F_3^l(\varphi, k)$  be defined from  $g_{\nu\alpha\beta}^l$  as in (3)–(5), and similarly make  $F_1^r$ ,  $F_2^r$  and  $F_3^r$  using  $g_{\nu\alpha\beta}^r$ .

By the invariance of the Alexander polynomial, the pre-factor  $\Delta_1 \Delta_2 \Delta_3$  is the same for  $\theta(D^l)$  and for  $\theta(D^r)$  (see Equation (6)). By Theorem 6,  $g_{\nu\alpha\beta}^l = g_{\nu\alpha\beta}^r$  so long as  $\alpha, \beta \notin \{i^+, j^+, k^+\}$ . And so the only terms that may differ in  $\theta(D^h)$  between  $h = l$  and  $h = r$  are the terms

$$A^h = \sum_{c \in \{c_{1,2,3}^h\}} F_1^h(c) + \sum_{c_0, c_1 \in \{c_{1,2,3}^h\}} F_2^h(c_0, c_1), \quad B^h = \sum_{c_0 \in \{c_{1,2,3}^h\}, c_y \in Y} F_2^h(c_0, c_y), \quad \text{and} \quad C^h = \sum_{c_1 \in \{c_{1,2,3}^h\}, c_y \in Y} F_2^h(c_y, c_1). \quad (16)$$

We claim that  $A^l = A^r$ ,  $B^l = B^r$ , and  $C^l = C^r$ .

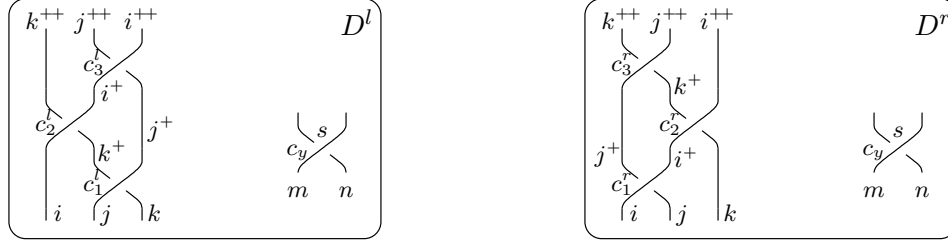


FIGURE 4.4. The two sides  $D^l$  and  $D^r$  of the R3b move. The left side  $D^l$  consists of 3 distinguished crossings  $c_1^l = (1, j, k)$ ,  $c_2^l = (1, i, k^+)$ ,  $c_3^l = (1, i^+, j^+)$  and a collection of further crossings  $c_y = (s, m, n) \in Y$ , where  $Y$  is the set of crossings not participating in the R3b move. The right side  $D^r$  consists of  $c_1^r = (1, i, j)$ ,  $c_2^r = (1, i^+, k)$ ,  $c_3^r = (1, j^+, k^+)$  and the same set  $Y$  of further crossings  $c_y$ .

fig:R3

To show that  $A^l = A^r$ , we need to compare polynomials in  $g_{\nu\alpha\beta}^l$  with polynomials in  $g_{\nu\alpha\beta}^r$  in which  $\alpha$  and  $\beta$  may belong to the set  $\{i^+, j^+, k^+\}$  on which it may be that  $g^l \neq g^r$ . Fortunately the  $g$ -rules of Equations (7) and (8) allow us to rewrite the offending  $g$ 's, namely the ones with subscripts in  $\{i^+, j^+, k^+\}$ , in terms of other  $g$ 's whose subscripts are in  $\{i, j, k, i^{++}, j^{++}, k^{++}\}$ , where  $g^l = g^r$ . So it is enough to show that

$$\text{under } g^l = g^r, \quad A^l /. (\text{the } g\text{-rules for } c_1^l, c_2^l, c_3^l) = A^r /. (\text{the } g\text{-rules for } c_1^r, c_2^r, c_3^r), \quad (17)$$

eq:R3A

where the symbol  $/.$  means “apply the rules”. This is a finite computation that can in principle be carried out by hand. But each  $A^h$  is a sum of  $3+9=12$  polynomials in the  $g^h$ 's, these polynomials are rather unpleasant (see (3) and (4)), and applying the relevant  $g$ -rules adds a bit further to the complexity. Luckily, we can delegate this pages-long calculation to an entity that works accurately and doesn't complain.

First, we implement the Kronecker  $\delta$ -function, the  $g$ -rules for a crossing  $(s, i, j)$ , and the  $g$ -rules for a list of crossings  $X$ :

```

(⊙) δi,j := If[i == j, 1, 0];
(♥) gRules[{s_, i_, j_}] := {
  gv,jβ => gv,j+β + δjβ, gv,iβ => Tvs gv,i+β + (1 - Tvs) gv,j+β + δiβ,
  gv,αi+ => Tvs gv,αi + δαi+, gv,αj+ => gv,αj + (1 - Tvs) gv,αi + δαj+
};
gRules[X__List] := Union@@Table[gRules[c], {c, {X}}]

```

We then let  $X1$  be the three crossings in the left-hand-side of the R3b move, as in Figure 4.4, we let  $A1$  be the  $A^l$  term of (16), and we let  $lhs$  be the result of applying the  $g$ -rules for the crossings in  $X1$  to  $A1$ . We print only a “Short” version of  $lhs$  because the full thing would cover about 2.5 pages:

```

(⊙) X1 = {{1, j, k}, {1, i, k+}, {1, i+, j+}};
(♥) A1 = Sum[F1[c], {c, X1}] + Sum[F2[c0, c1], {c0, X1}, {c1, X1}];
lhs = Simplify[A1 //. gRules @@ X1];
Short[lhs, 5]

```

fig:R3

eq:ABC

$$\begin{aligned}
& - \frac{1}{2(1-T_2)} \left( 3 - 3T_2 + \ll 129 \gg + \right. \\
& \quad 2(1-T_2) \left( 1 + T_2 (T_2 g_{2, \ll 1 \gg^+, i} - (-1 + T_2) g_{2, \ll 1 \gg, i}) - (-1 + T_2) g_{2, (k^+)^+, i} \right) \\
& \quad \left. (1 + (1 - T_1 T_2) g_{3, (k^+)^+, j} + g_{3, (k^+)^+, k}) \right)
\end{aligned}$$

We do the same for  $A^r$ , except this time, without printing at all:

```

-- Xr = {{1, i, j}, {1, i+, k}, {1, j+, k+}};
-- Ar = Sum[F1[c], {c, Xr}] + Sum[F2[c0, c1], {c0, Xr}, {c1, Xr}];
-- rhs = Simplify[Ar //. gRules @@ Xr];

```

We then compare lhs with rhs. The output, True, tells us that we have proven (17): leg:R3A

```

-- Simplify[lhs == rhs]

```

True

We show that  $B^l = B^r$  by following exactly the same procedure. Note that we ignore the summation over  $c_y$  and instead treat  $c_y$  as a fixed crossing  $(s, m, n)$ . If an equality is proven for every fixed  $c_y$ , it is of course also proven for the sum over  $c_y \in Y$ .

```

-- lhs = Sum[F2[c0, {s, m, n}], {c0, Xl}] //. gRules @@ Xl;
-- rhs = Sum[F2[c0, {s, m, n}], {c0, Xr}] //. gRules @@ Xr;
-- Simplify[lhs == rhs]

```

True

Similarly we prove that  $C^l = C^r$ , and this concludes the proof of Proposition 8. prop:R3

```

-- lhs = Sum[F2[{s, m, n}, c1], {c1, Xl}] //. gRules @@ Xl;
-- rhs = Sum[F2[{s, m, n}, c1], {c1, Xr}] //. gRules @@ Xr;
-- Simplify[lhs == rhs]

```

True

rem:E

**Remark 9.** The computations above were carried out for generic  $g_{\nu\alpha\beta}$  and for a generic  $c_y = (s, m, n)$ ; namely, without specifying the knot diagrams in full, and hence without assigning specific values to  $g_{\nu\alpha\beta}$ , and without specifying  $m$  and  $n$ . Under these conditions the three parts of (16) cannot mix (namely, terms from, say,  $A^h$  cannot cancel terms in  $B^h$  or  $C^h$ ), and so it would have been enough to show that  $E^l = E^r$ , where  $E^h$  combines  $A^h$  and  $B^h$  and  $C^h$  (and a few harmless further terms) by adding  $c_y$  to the summation corresponding to  $A^h$ : ed:ABC

$$E^h = \sum_{c \in \{c_{1,2,3,y}^h\}} F_1^h(c) + \sum_{c_0, c_1 \in \{c_{1,2,3,y}^h\}} F_2^h(c_0, c_1).$$

But that's a simpler computation:

```

-- ESum[X_] := (Sum[F1[c], {c, X}] + Sum[F2[c0, c1], {c0, X}, {c1, X}]) //. gRules @@ X;

```

```

-- Xl = {{1, j, k}, {1, i, k+}, {1, i+, j+}};
-- Xr = {{1, i, j}, {1, i+, k}, {1, j+, k+}};
-- Simplify[ESum[Append[Xl, {s, m, n}]] == ESum[Append[Xr, {s, m, n}]]]

```

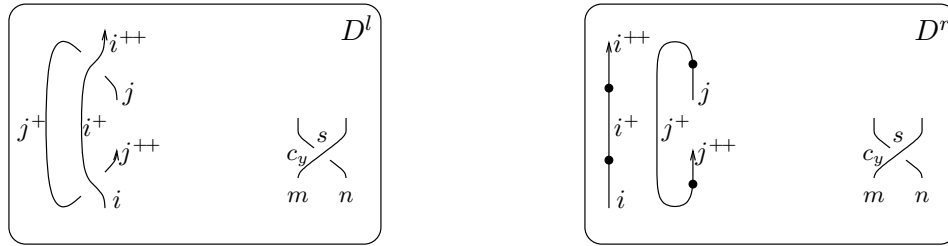
True

rem:E  
9

**Proposition 10.** The quantity  $\theta$  is invariant under the upright  $R2c^+$  and  $R2c^-$ . prop:R2c

*Proof.* For  $R2c^+$  we follow the same logic as in the proof of Proposition 8, as simplified by Remark 9. We start with the figure that replaces Figure 4.4 (note the null vertices in  $D^r$  fig:R3) prop:R3

and their minimal effect as in Lemma 4 and Remark 5):



To compute “ $E$ ” sums as in Remark 9 we first have to extend the `ESum` routine to accept also a list  $R$  of pairs  $(\varphi, k)$  of the form (rotation number, edge label):

```

-- ESum[X_, R_] :=
-- (Sum[F1[c], {c, X}] + Sum[F2[c0, c1], {c0, X}, {c1, X}] + Sum[F3@@r, {r, R}]) /.
-- gRules @@ X;

```

We then compute  $E^l$  by calling `ESum` with crossings  $(-1, i, j^+)$ ,  $(1, i^+, j)$  as in the left hand side of the  $R2c^+$  moves, a generic extra crossing  $(s, m, n)$ , and a rotation number of 1 on edge  $j^+$ :

```

-- E1 = Simplify[ESum[{{-1, i, j^+}, {1, i^+, j}, {s, m, n}}, {{1, j^+}}]];
-- Short[E1, 5]

```

$$\begin{aligned}
& -\frac{1}{2(-1 + T_2^S)} \left( (1 + s + 2s(T_1 T_2)^S g_{3,m^+,m} + \ll 11 \gg + 2g_{3,(j^+)^+,j} - \right. \\
& \quad \left. T_2^S (1 + s - 2s g_{1,n^+,m} g_{2,n^+,m} + 2s g_{2,n^+,n} + \ll 28 \gg + 2s g_{2,m^+,m} (1 + g_{3,n^+,n}) + 2g_{3,(j^+)^+,j}) \right)
\end{aligned}$$

The computation of  $E^r$  is simpler, as it only involves the generic  $(s, m, n)$  and the rotation  $(1, j^+)$ . We implement the  $g$ -rules for null vertices as in Equations (10) and (11), compute  $E^r$ , and then compare  $E^l$  with  $E^r$  to conclude the invariance under  $R2c^+$ :

```

-- gRules[j_] := {g_{v-,j,\beta_-} \Rightarrow \delta_{j,\beta} + g_{v,j^+,\beta}, g_{v-,a-,j^+} \Rightarrow \delta_{a,j^+} + g_{v,a,j}}
-- Er = ESum[{{s, m, n}}, {{1, j^+}}] /. (Union@@gRules /@ {i, i^+, j, j^+});
-- Simplify[E1 == Er]

```

```

-- True

```

For  $R2c^-$  we allow ourselves to be even more condensed:

```

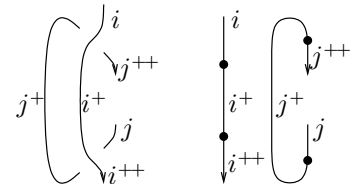
-- E1 = ESum[{{1, i, j^+}, {-1, i^+, j}, {s, m, n}}, {{-1, j^+}}];
-- Er = ESum[{{s, m, n}}, {{-1, j^+}}] /.
-- (Union@@gRules /@ {i, i^+, j, j^+});
-- Simplify[Er == E1]

```

```

-- True

```



prop:R1s

**Proposition 11.** *The quantity  $\theta$  is invariant under R1l and R1r.*

*Proof.* We aim to use the same approach and conventions as in the previous two proofs but hit a minor snag. The  $g$ -rules for R1l include

$$g_{i+\beta} = \delta_{i+\beta} + T g_{i^{++},\beta} + (1-T) g_{i^+,\beta} \quad \text{and} \quad g_{\alpha,i^+} = g_{\alpha i} + (1-T) g_{\alpha i^+} + \delta_{\alpha,i^+},$$

and if these are implemented as simple left to right replacement rules, they lead to infinite recursion. Fortunately, these rules can be rewritten in the form

$$g_{i+\beta} = T^{-1} \delta_{i+\beta} + g_{i^{++},\beta} \quad \text{and} \quad g_{\alpha,i^+} = T^{-1} g_{\alpha i} + T^{-1} \delta_{\alpha,i^+},$$

which makes perfectly valid replacement rules. We thus redefine:

```

gRules[{1, i+, i}] = {
  gviβ- := gvi+β + δiβ, gvi+β- := gv(i+)+β + T-1 δi+β,
  gvα-(i+)+ := Tv gvαi+ + δα(i+)+, gvα-i+ := Tv-1 gvαi + Tv-1 δαi+
};

```

The same issue does not arise for R1r (!), and thus the following lines conclude the proof:

```

E1 = ESum[{1, i+, i}, {s, m, n}, {{1, i+}}];
Em = ESum[{s, m, n}];
Er = ESum[{1, i, i+}, {s, m, n}, {{-1, i+}}];
Simplify[E1 == Em == Er]

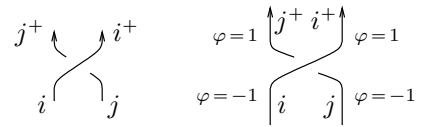
```

 True
prop:R1s  
11

prop:Sw

**Proposition 12.** *The quantity  $\theta$  is invariant under Sw.*

*Proof.* This one is routine:



```

E1 = ESum[{1, i, j}, {s, m, n}];
Er = ESum[{1, i, j}, {s, m, n}, {{-1, i}, {-1, j}, {1, i+}, {1, j+}}];
Simplify[E1 == Er]

```

 True
prop:Sw  
12

prop:NV

**Proposition 13.** *The quantity  $\theta$  is invariant under NV.*




*Proof.* Indeed,  $F_3$  is linear in  $\varphi$ .

*Proof of Theorem 2.* Theorem 2 now follows from Propositions 7, 8, 10, 11, 12, and 13.

□  
□





1	$n$	$\leq 10$	$\leq 11$	$\leq 12$	$\leq 13$	$\leq 14$	$\leq 15$
2	knots	249	801	2,977	12,965	59,937	313,230
3	$\Delta$	(38)	(250)	(1,204)	(7,326)	(39,741)	(236,326)
4	$J$	(7)	(70)	(482)	(3,434)	(21,250)	(138,591)
5	$Kh$	(6)	(65)	(452)	(3,226)	(19,754)	(127,261)
6	$H$	(2)	(31)	(222)	(1,839)	(11,251)	(73,892)
7	$Vol$	(~6)	(~25)	(~113)	(~1,012)	(~6,353)	(~43,607)
8	$(Kh, H, Vol)$	(~0)	(~14)	(~84)	(~911)	(~5,917)	(~41,434)
9	$(\Delta, \rho_1)$	(0)	(14)	(95)	(959)	(6,253)	(42,914)
10	$(\Delta, \rho_1, \rho_2)$	(0)	(14)	(84)	(911)	(5,926)	(41,469)
11	$(\rho_1, \rho_2, Kh, H, Vol)$	(0)	(~14)	(~84)	(~911)	(~5,916)	(~41,432)
12	$\Theta$	(0)	(3)	(19)	(194)	(1,118)	(6,758)
13	$(\Theta, \rho_2)$	(0)	(3)	(10)	(169)	(982)	(6,341)
14	$(\Theta, Kh)$	(0)	(3)	(18)	(185)	(1,062)	(6,555)
15	$(\Theta, H)$	(0)	(3)	(18)	(185)	(1,064)	(6,563)
16	$(\Theta, Vol)$	(0)	(~3)	(~10)	(~169)	(~973)	(~6,308)
17	$(\Theta, \rho_2, Kh, H, Vol)$	(0)	(~3)	(~10)	(~169)	(~972)	(~6,304)

TABLE 5.1. The separation powers of some knot invariants and combinations of knot invariants (in lines 3–17, smaller numbers are better). The data in this table was assembled by [BV3, Stats.nb].

## 5. STRONG AND MEANINGFUL

5.1. **Strong.** To illustrate the strength of  $\Theta$ , Table 5.1 summarises the separation powers of various knot invariants and combinations of knot invariants on prime knots with up to 15 crossings (up to reflections and reversals).

In line 2 of the table we list the total number of tabulated knots with up to  $n$  crossings. For example, there are 313,230 prime knots up to reflections and reversals with at most 15 crossings. In the following lines we list the *separation deficits* on these knots, for different invariants or combinations of invariants. For example, in line 3 we can see that on knots with up to 10 crossings, the Alexander polynomial  $\Delta$  has a separation deficit of 38: meaning, that it attains  $249 - 38 = 211$  distinct values on the 249 knots with up to 10 crossings. For deficits, the smaller the better!<sup>3</sup> Thus the deficit of 236,326 for  $\Delta$  at  $n \leq 15$  means that the Alexander polynomial is a rather weak invariant, in as much as separation power is concerned.

Line 4 shows the deficits for the Jones polynomial  $J$ . It is better than  $\Delta$ , but still rather weak. Line 5 shows the deficits for Khovanov homology  $Kh$ . They are only a bit lower than those of  $J$ . On line 6, the HOMFLY-PT polynomial  $H$  is noticeably better.

On line 7 we consider the hyperbolic volume  $Vol$  of the knot complement, as computed by SnapPy [CDGW]. We computed volumes using SnapPy's `high_precision` flag, which makes SnapPy compute to roughly 63 decimal digits, and then truncated the results to 58 decimal digits to account for possible roundoff errors within the last few digits. But then we are unsure if we computed enough.... Hence the uncertainty symbols “~” on some of

<sup>3</sup>This is not a political statement.

✓ 0 is TL...

the results here and in the other lines that contain  $Vol$ . This said,  $Vol$  seems to be the champion so far.

Line 8 is “everything so far, taken together”. Note that  $Kh$  dominates  $J$  and  $H$  dominates both  $\Delta$  and  $J$ , so there’s no point adding  $\Delta$  and/or  $J$  into the mix.

On line 9, the Rozansky-Overbay invariant  $\rho_1$  [Ro1, Ro2, Ro3, Ov], also discussed by us in [BV1], does somewhat better. Note that the computation of  $\Delta$  is a part of the computation of  $\rho_1$ , so we always take them together. In line 10 we add  $\rho_2$  [BN2] to make the results yet a bit better.

Line 11 is “everything before  $\Theta$ ”.

Line 12 makes our case that  $\Theta$  is strong — the deficit here, for knots with up to 15 crossings, is about a sixth of the deficit in line 11!

Line 13 reinforces our case by just a bit: note that it makes sense to bundle  $\rho_2$  along with  $\Theta$ , for their computations are very similar. Note also that Conjecture 18 means that it is pointless to consider  $(\Theta, \rho_1)$ .

Lines 14 through 16 show that at crossing number  $\leq 15$  and in the presence of  $\Theta$ , and especially in the presence of both  $\Theta$  and  $\rho_2$ , it is pointless to also consider  $H$  or  $Kh$ , and only mildly useful to also consider  $Vol$ . Line 17 shows that once  $Vol$  has been added to  $\Theta$ , the other invariants contribute almost nothing.

We note that of all the invariants considered in this section, the only one known to (sometimes) detect knot mutation is  $\Theta$  (see Section 3.2).

**5.2. Meaningful.** Many knot polynomials have some separation power, some more and some less, yet they seem to “see” almost no other topological properties of knots. The greatest exception is the Alexander polynomial, which despite having rather weak separation powers, gives a genus bound, a fiberness condition, and a ribbon condition. The definition of  $\theta$  is in some sense “near” the definition of  $\Delta$ , and one may hope that  $\theta$  will share some of the good topological properties of  $\Delta$ . With significant computational and theoretical (see also MORE) evidence we believe the following to be true:

**Conjecture 14.** Let  $K$  be a knot and  $g(K)$  the genus of  $K$ . Then  $\deg_{T_1} \theta(K) \leq 2g(K)$ .

B. Line 13.5 shows that  $\Theta$  dominates  $\sigma$ , at least for knots with up to 15 crossings. We don't know why this is so. From further computations in [ ] we know that the triple  $(Kh, H, Vol)$  also dominates  $\sigma$  for knots with up to 15 crossings, yet individually, each of  $Kh$ ,  $H$ , and  $Vol$  does not. We don't know why this is so.





## 6. STORIES, CONJECTURES, AND DREAMS

There is a story teller in each of us, who wants to tell a coherent story, with a beginning, a middle, and an end. Unfortunately of us, the  $\Theta$  story isn't that neat. Calling the content of the first few sections of this paper "the middle", we are quite unsure about the beginning and the end. The "beginning" can be construed to mean "the thought process that lead us here". But that process was too long and roundabout to be given in full here (though much of it can be gleaned by reading this section). What's worse, we believe that ultimately, our peculiar thought process will be replaced by much more solid foundations and motivations, perhaps along the lines of Dreams ?? and ??. ~~As~~ this solid foundation is not available yet, even if we are working hard to expose it. As for the end of the story, it is clearly not known yet.

Hence this section is a bit sketchy and disorganized. Those facts that we already know, those conjectures we believe in, and the dreams we dream, are all here in some random order. But the narrative is lacking.

**Conjecture 15.**  $\theta$  has hexagonal symmetry. That is, for any knot  $K$ , we have that  $\theta = \theta|_{T_1 \rightarrow T_1, T_2 \rightarrow T_1^{-1} T_2^{-1}}$  ("the QR code is invariant under reflection about a horizontal line"), and  $\theta = \theta|_{T_1 \rightarrow T_1 T_2, T_2 \rightarrow T_2^{-1}}$  ("the QR code is invariant under reflection about the line of slope  $30^\circ$ ").

The Alexander polynomial has a simpler symmetry,  $\Delta = \Delta|_{T \rightarrow T^{-1}}$ . It is rather difficult to deduce the symmetry of  $\Delta$  from the formula in this paper, Equation (2) (though it is possible; once notational differences are overcome, the proof is e.g. in [CF, Chapter IX]). Instead, the standard proof of the symmetry of  $\Delta$  uses the Seifert surface formula for  $\Delta$  (e.g. [Li, Chapter 6]). We expect that Conjecture 15 will be proven as soon as a Seifert formula is found for  $\theta$ . See Dream ?? below.

**Conjecture 16.** If  $\bar{K}$  denotes the mirror image of a knot  $K$ , then  $\theta(\bar{K}) = -\theta(K)$ .

**Conjecture 17.** If  $-K$  denotes the reverse of a knot  $K$  (namely,  $K$  taken with the opposite orientation), then  $\theta(-K) = \theta(K)$ .

**Conjecture 18.**  $\theta$  dominates the Rozansky-Overbay invariant  $\rho_1$  [Ro1, Ro2, Ro3, Ov], also discussed by us in [BV1]. In fact,  $\rho_1 = -\theta|_{T_1 \rightarrow T, T_2 \rightarrow 1}$ .

**Conjecture 19.**  $\theta$  is equal to the "two-loop polynomial" studied extensively by Ohtsuki [Oh2], continuing Rozansky, Garoufalidis, and Kricker [GR, Ro1, Ro2, Ro3, Kr].

**Discussion 20.** People who are already familiar with "the loop expansion" may consider the above conjecture an "explanation" of  $\theta$ . We differ. An elementary construction ought to have a simple explanation, and the loop expansion is too complicated to be that.

Be it as it may, Ohtsuki [Oh2] shows that Conjecture 19 implies Conjectures 14, 15, 16, and 17.

Next, let us briefly sketch some key points from [BN1, BV2], where we explain how to obtain poly-time computable knot invariants from certain Lie algebraic constructions.

**Discussion 21.** Let  $\mathfrak{g}$  be a semi-simple Lie algebra, let  $\mathfrak{b}$  be its upper Borel subalgebra, and let  $\mathfrak{h}$  be its Cartan subalgebra. Then  $\mathfrak{b}$  has a Lie bracket  $\beta$  and, as the dual of the lower Borel subalgebra, it also has a cobracket  $\delta$ . It turns out that  $\mathfrak{g}$  can be recovered from the triple  $(\mathfrak{b}, \beta, \delta)$ ; in fact,  $\mathfrak{g}^+ := \mathfrak{g} \oplus \mathfrak{h} \simeq \mathcal{D}(\mathfrak{b}, \beta, \delta)$ , where  $\mathcal{D}$  denotes the Manin double construction<sup>4</sup>. We now set  $\mathfrak{g}_\epsilon^+ := \mathcal{D}(\mathfrak{b}, \beta, \epsilon\delta)$ , where  $\epsilon$  is a formal "small" parameter. The family  $\mathfrak{g}_\epsilon^+$  is a



1-parameter family of Lie algebras all defined on the same underlying vector space  $\mathfrak{b} \oplus \mathfrak{b}^*$ . If  $\epsilon$  is invertible then  $\mathfrak{g}_\epsilon^+$  is independent of  $\epsilon$  and is always isomorphic to  $\mathfrak{g}^+ = \mathfrak{g}_1^+$ . Yet at  $\epsilon = 0$ ,  $\mathfrak{g}_0^+$  is solvable, and as the name “solvable” suggests, computations in  $\mathfrak{g}_0^+$  can be “solved”.

Hence in [BN1, BV2], mostly in the case where  $\mathfrak{g} = \mathfrak{sl}_2$ , we use the Drinfeld double construction to quantize the universal enveloping algebra  $\mathcal{U}(\mathfrak{g}^+)$  and use it to define a “universal quantum invariant”  $Z_\epsilon^\mathfrak{g}$  (in the sense of [La, Oh1]). We then expand  $Z_\epsilon^\mathfrak{g}$  near where it’s easy; namely, as a power series around  $\epsilon = 0$ . In the case of  $\mathfrak{g} = \mathfrak{sl}_2$ , and almost certainly in general, we write  $Z_\epsilon^\mathfrak{g} = \rho_0^\mathfrak{g} \exp(\sum_{d \geq 1} \rho_d^\mathfrak{g} \epsilon^d)$  and find that we can interpret the  $\rho_d^\mathfrak{g}$  as polynomials in as many variables as the rank of  $\mathfrak{g}$ . It turns out that  $\rho_0^\mathfrak{g}$  is always determined by the Alexander polynomial and the  $\rho_d^\mathfrak{g}$  are always computable in polynomial time (with polynomials whose exponent and coefficients get worse as  $d$  grows bigger and  $\mathfrak{g}$  gets more complicated).

Our papers and talks [BV1, BV2, BN2] carry out the above procedure in the case where  $\mathfrak{g} = \mathfrak{sl}_2$ , calling the resulting invariants  $\rho_d$ , for  $d \geq 1$ . They are the same as  $\rho_1$  and  $\rho_2$  of Section 5.1.

Following some preliminary work by Schaveling [Sch], in the summer of 2024 we’ve set out to find good formulas for  $\rho_1^{\mathfrak{sl}_3}$ . Tracing Discussion 21 seemed technically hard, so instead, we extracted from the procedure the “shape” of the formulas we could expect to get and, and then we found the invariant  $\theta$  by the method of undetermined coefficients assisted by some difficult-to-formulate intuition. Thus our formulas for  $\theta$  arose from our expectations for  $\rho_1^{\mathfrak{sl}_3}$ , and yet we have not proved that they are equal!

**Conjecture 22.** *Up to conventions and normalizations,  $\theta = \rho_1^{\mathfrak{sl}_3}$ .*

People who are versed with Lie algebras and their quantizations may consider the above an “explanation” of  $\theta$ , and may be looking forward to a more detailed exposition of  $\rho_d^\mathfrak{g}$ . We differ, for the same reasons as in Discussion 20. We expect the eventual “origin story” for  $\theta$  to be simpler and more natural.

MORE

<sup>4</sup>We are unsure about naming.  $\mathcal{D}$  is also known as “the Drinfeld double” construction for Lie bialgebras (as opposed to Hopf algebras). Yet when Drinfeld first refers to this construction in [Dr], in reference to Lie bialgebras, he repeatedly names it after Manin (under the less clear name “Manin triples”), yet without providing a reference.

## REFERENCES

- [Al] J. W. Alexander, *Topological invariants of knots and link*, Trans. Amer. Math. Soc. **30** (1928) 275–306. See pp. 3.
- [BN1] D. Bar-Natan, *Everything around  $sl_{2+}^{\epsilon}$  is DoPeGDO. So what?*, talk given in “Quantum Topology and Hyperbolic Geometry Conference”, Da Nang, Vietnam, May 2019. Handout and video at [omega-beta/DPG](http://drorbn.net/omega-beta/DPG). See pp. 31, 32.
- [BN2] D. Bar-Natan, *Cars, Interchanges, Traffic Counters, and some Pretty Darned Good Knot Invariants*, talk given in Oaxaca, October 2022. Video and handout at <http://drorbn.net/oa22>. See pp. 18, 19, 28, 32.
- [BN3] Dror Bar-Natan, *Knot Invariants from Finite Dimensional Integration*, talks in Beijing (July 2024, <http://drorbn.net/icbs24>), Geneva (August 2024, <http://drorbn.net/ge24>) and Bonn (May 2025, <http://drorbn.net/bo25>). See pp. 8.
- [BN4] Dror Bar-Natan, *The Strongest Genuinely Computable Knot Invariant in 2024*, talk given in Toronto (October 2024, <http://drorbn.net/to24>). See pp. 8, 18, 19.
- [BV1] D. Bar-Natan and R. van der Veen, *A Perturbed-Alexander Invariant*, Quantum Topology **15** (2024) 449–472, [arXiv:2206.12298](https://arxiv.org/abs/2206.12298). See pp. 7, 8, 17, 18, 19, 28, 31, 32.
- [BV2] D. Bar-Natan and R. van der Veen, *Perturbed Gaussian Generating Functions for Universal Knot Invariants*, [arXiv:2109.02057](https://arxiv.org/abs/2109.02057). See pp. 31, 32.
- [BV3] D. Bar-Natan and R. van der Veen, *A Very Fast, Very Strong, Topologically Meaningful and Fun Knot Invariant*, (self-reference), paper and related files at <http://drorbn.net/Theta>. The [arXiv:????????](https://arxiv.org/abs/????????) edition may be older. See pp. 11, 14, 27.
- [BVH] J. Becerra and K. van Helden, *Minimal Generating Sets of Rotational Reidemeister Moves*, [arXiv:2506.15628](https://arxiv.org/abs/2506.15628). See pp. 21.
- [CF] R. H. Crowell and R. H. Fox, *Introduction to Knot Theory*, Springer-Verlag GTM **57** (1963). See pp. 31.
- [CDGW] M. Culler, N. Dunfield, M. Goerner, and J. Weeks, *SnapPy, a computer program for studying the geometry and topology of 3-manifolds*, <http://snappy.computop.org>. See pp. 27.
- [Dr] V. G. Drinfel’d, *Quantum Groups*, Proc. Int. Cong. Math., 798–820, Berkeley, 1986. See pp. 32.
- [DHOEBL] N. Dunfield, A. Hirani, M. Obeidin, A. Ehrenberg, S. Bhattacharyya, D. Lei, and others, *Random Knots: A Preliminary Report*, lecture notes at [https://nmd.web.illinois.edu/slides/random\\_knots.pdf](https://nmd.web.illinois.edu/slides/random_knots.pdf). Also a data file at [https://drorbn.net/AcademicPensieve/People/Dunfield/nmd\\_random\\_knots](https://drorbn.net/AcademicPensieve/People/Dunfield/nmd_random_knots). See pp. 5.
- [GR] S. Garoufalidis and L. Rozansky, *The Loop Expansion of the Kontsevich Integral, the Null-Move, and S-Equivalence*, [arXiv:math.GT/0003187](https://arxiv.org/abs/math.GT/0003187). See pp. 1, 31.
- [GST] R. E. Gompf, M. Scharlemann, and A. Thompson, *Fibered Knots and Potential Counterexamples to the Property 2R and Slice-Ribbon Conjectures*, Geom. and Top. **14** (2010) 2305–2347, [arXiv:1103.1601](https://arxiv.org/abs/1103.1601). See pp. 29.
- [Kr] A. Kriker, *The Lines of the Kontsevich Integral and Rozansky’s Rationality Conjecture*, [arXiv:math/0005284](https://arxiv.org/abs/math/0005284). See pp. 1, 31.
- [La] R. J. Lawrence, *Universal Link Invariants using Quantum Groups*, Proc. XVII Int. Conf. on Diff. Geom. Methods in Theor. Phys., Chester, England, August 1988. World Scientific (1989) 55–63. See pp. 32.
- [Li] W. B. R. Lickorish, *An Introduction to Knot Theory*, Springer-Verlag GTM **175** (1997). See pp. 31.
- [Oh1] T. Ohtsuki, *Quantum Invariants*, Series on Knots and Everything **29**, World Scientific 2002. See pp. 32.
- [Oh2] T. Ohtsuki, *On the 2-Loop Polynomial of Knots*, Geometry & Topology **11** (2007) 1357–1475. See pp. 1, 31.
- [Ov] A. Overbay, *Perturbative Expansion of the Colored Jones Polynomial*, Ph.D. thesis, University of North Carolina, August 2013, <https://cdr.lib.unc.edu/concern/dissertations/hm50ts889>. See pp. 28, 31.
- [Po] M. Polyak, *Minimal Generating Sets of Reidemeister Moves*, Quantum Topol. **1** (2010) 399–411, [arXiv:0908.3127](https://arxiv.org/abs/0908.3127). See pp. 19.

ntribution

- [Ro1] L. Rozansky, *A Contribution of the Trivial Flat Connection to the Jones Polynomial and Witten's Invariant of 3D Manifolds, I*, Comm. Math. Phys. **175-2** (1996) 275–296, [arXiv:hep-th/9401061](https://arxiv.org/abs/hep-th/9401061). See pp. [1](#), [28](#), [31](#).

nsky:Burau

- [Ro2] L. Rozansky, *The Universal R-Matrix, Burau Representation and the Melvin-Morton Expansion of the Colored Jones Polynomial*, Adv. Math. **134-1** (1998) 1–31, [arXiv:q-alg/9604005](https://arxiv.org/abs/q-alg/9604005). See pp. [1](#), [28](#), [31](#).

nsky:U1RCC

- [Ro3] L. Rozansky, *A Universal  $U(1)$ -RCC Invariant of Links and Rationality Conjecture*, [arXiv:math/0201139](https://arxiv.org/abs/math/0201139). See pp. [1](#), [28](#), [31](#).

ing:Thesis

- [Sch] S. Schaveling, *Expansions of Quantum Group Invariants*, Ph.D. thesis, Universiteit Leiden, September 2020, <https://scholarlypublications.universiteit leiden.nl/handle/1887/136272>. See pp. [32](#).

athematica

- [Wo] *Wolfram Language & System Documentation Center*, <https://reference.wolfram.com/language/>. See pp. [11](#).

DEPARTMENT OF MATHEMATICS, UNIVERSITY OF TORONTO, TORONTO ONTARIO M5S 2E4, CANADA

*Email address:* [drorbn@math.toronto.edu](mailto:drorbn@math.toronto.edu)

*URL:* <http://www.math.toronto.edu/drorbn>

UNIVERSITY OF GRONINGEN, BERNOULLI INSTITUTE, P.O. Box 407, 9700 AK GRONINGEN, THE NETHERLANDS

*Email address:* [roland.mathematics@gmail.com](mailto:roland.mathematics@gmail.com)

*URL:* <http://www.rolandvdv.nl/>